Size-dependent electronic and optical properties of GaN nanotubes studied using LDA calculations

B. Xu and B. C. Pan
Hefei National Laboratory for Physical Sciences at Microscale and Department of Physics, University of Science and Technology of China, Hefei, Anhui 230026, People's Republic of China
(Received 14 May 2006; revised manuscript received 15 October 2006; published 1 December 2006)

The electronic structures and optical properties of GaN nanotubes are studied by using density functional theory with the generalized gradient approximation. Our calculations find that the threefold-coordinated N and Ga atoms at lateral facets in a GaN nanotube give rise to defect states near the top of valence band and the bottom of conduction band, respectively. Moreover, the calculated imaginary parts of dielectric functions, ϵ_2, show two significant peaks that, respectively, originate from the surface atoms and the bulk atoms. We find that the former peak shows a redshift and the latter shows a blueshift with respect to the major peak in the ϵ_2 curve of a wurtzite GaN. It is observed from the ϵ_2 curves that, as the thickness of GaN nanotubes increases, the intensity of the peak associated with the threefold-coordinated atoms decreases, while that associated with the bulk atoms is enhanced relatively. When the thickness of a GaN nanotube is large enough, the former peak vanishes nearly and the latter one tends to the case of a wurtzite GaN. We therefore predict that the absorption spectra of realistic GaN nanotubes with large thickness are most probably associated with the electronic states of the bulk portions of the tubes.

DOI: 10.1103/PhysRevB.74.245402 PACS number(s): 78.20.Ci, 73.22.−f, 71.15.Mb

I. INTRODUCTION

So far, scientists have revealed that the electronic properties of a single-walled carbon nanotube (SWNT) are sensitively dependent on its radius and chirality.[1–4] For a multiwalled carbon nanotube (MWNT), however, owing to the very weak interaction between the adjacent coaxial SWNT's, the electronic properties rely upon the individual coaxial SWNT's in it predominantly.[5–7] So the thickness of a MWNT is not a critical factor subject to its intrinsic electronic structures. However, the thickness of a single-crystal nanotube with periodic structure along its axial direction and finite crystal in its radial direction plays a significant role in the electronic and optical properties. For example, recent experiment found[8] that the optical spectra of single-crystal GaN nanotubes exhibit a blueshift slightly relative to that of bulk GaN. Such a blueshift basically results from the surface effect and/or quantum-size effect related to the thickness of the single-crystal GaN nanotubes.

On the other hand, the emissions ranging from 360 nm to 375 nm observed in the optical spectra[8] all originated from the band edge; no midgap emission has been observed for synthesized single-crystal GaN nanotubes yet. This finding shows that atoms in surfaces of single-crystal GaN nanotubes do not cause any midgap state probably. Essentially, these phenomena are associated with the bonding characters of the atoms at the surfaces of the tubes. Therefore, to understand the experimental results,[8] it is necessary to investigate the atomic structures and the related electronic structures of GaN nanotubes.

In this paper, we systematically calculate the electronic structures and the imaginary parts of the dielectric functions for GaN nanotubes with different thicknesses. We find that the threefold-coordinated N and Ga atoms at lateral facets in a tube give rise to defect states at the valence-band edge and conduction-band edge near the band gap, respectively. Moreover, the calculated ϵ_2 curves of the concerned tubes show a significant size dependence.

II. ATOMIC STRUCTURES OF GaN NANOTUBES

Previously, we proposed an approach to construct single-crystal GaN nanotubes from wurtzite (WZ) GaN.[9] That is, a hexagonal cylinder with the [0001] axial direction in a wurtzite GaN is isolated, and then a coaxial hexagonal cylinder with smaller diameter is removed from the isolated hexagonal cylinder. The residual is a GaN nanotube with hexagonal cross section. Employing this scheme, in this work, we generate three GaN nanotubes, which consist of one, two, and three double atomic layers, respectively. For these tubes, the lateral facets are all oriented in the $[10\bar{1}0]$ direction. For convenience, the tubes above are, respectively, named H-1, H-2, and H-3.

The nanotubes generated above are fully optimized by using the SIESTA code[10] with a double-ζ basis set and generalized gradient approximation (GGA) with Perdew-Burke-Ernzerhof exchange-correlation functional.[11] The lattice constant along the axis of each tube is set to be 5.34 Å. The number of atoms in each unit cell for the H-1, H-2, and H-3 tubes is 36, 96, and 180, respectively. In addition, 11 *K*-sampling points in an irreducible Brillouin zone are utilized in our calculations.

Our calculations find that the puckered cross section of the initial H-1 tube changes into a circle after relaxation [seen in Fig. 1(a)]. This relaxed tube is actually single-walled, where each atom bonds with its three nearest atoms, being the same as that reported by Lee *et al.*[12] and Wang *et al.*[13] For the H-2 tube, optimization results in the breaking of some Ga-N bonds between the two double layers [Fig. 1(b)], where only a few atoms bridge the two double layers. These bridging atoms are fourfold coordinated, being analo-

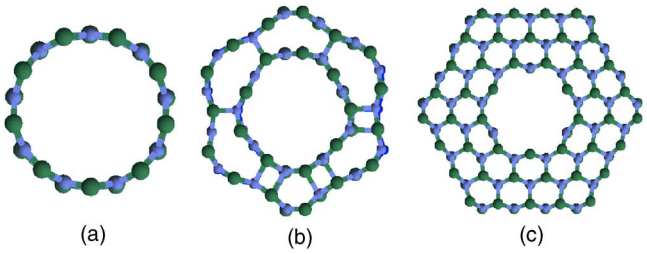

FIG. 1. (Color online) The structural models of GaN nanotubes with hexagonal cross section. (a), (b), and (c) represent the GaN nanotubes with one, two, and three double atomic layers, respectively. The large balls (in green blue) stand for the Ga atoms and the small balls (in blue) for the N atoms.

gous to the atoms in bulk WZ GaN somewhat. For the GaN nanotube (H-3) with three double layers, the optimal structure [Fig. 1(c)] is almost the same as its initial one. In this case, there are many atoms to have the same bonding character as that of the bulk WZ GaN. So this tube contains more information of the bulk GaN than the H-2 tube. Additionally, it is noted that there is a dangling bond on each atom at the lateral facets for all of the GaN nanotubes. These dangling bonds should contribute to the electronic structures of the tubes to some extent.

III. ELECTRONIC PROPERTIES

As a reference, the band structure of a WZ GaN is calculated first, from which the width of band gap is evaluated to be about 2.3 eV, being smaller than the experimental value.[14] Then, the band structures of the H-1, H-2, and H-3 tubes are calculated. It is observed that these tubes are all semiconducting, with band gaps of 3.7 eV, 2.8 eV, and 2.5 eV, respectively. These band gaps are larger than that of the WZ GaN. Such a semiconducting feature of the GaN nanotubes predicted in our calculations is consistent with recent theoretical calculations.[13] It is noted that the calculated band gap decreases as the thickness of the GaN nanotube increases, showing a size effect clearly. Furthermore, that the band gap becomes narrow mainly results from a downshift of conduction-band minimum, while the valence-band maximum seems to be not sensitive to a change of the thickness of the tube. A similar scenario was observed in the mixed phase of silicon with different-sized inclusions.[15] We emphasize that our calculations could not find any midgap state in the band-gap regions of the GaN nanotubes, consistent with the observation in experiment.[8] In order to arrive at a deep understanding of the features in the band edges near the band gaps, we compute the total density of states (TDOS) and partial density of states (PDOS) of representative atoms in each system, as plotted in Fig. 2. For comparison, the TDOS and PDOS of the bulk GaN are also calculated and the obtained PDOS shows that the edges of the valence and conduction bands near the band gap characterize a hybridization of atomic orbitals from the Ga and N atoms [Fig. 2(a)]. Moreover, the major components in the top of the valence band are contributed from the N atoms, whereas those in the edge of the conduction band are mainly from the Ga atoms.

The calculated TDOS of the H-1 tube [Fig. 2(b)] is distinct from that of a bulk WZ GaN. There is a sharp peak ($S2$) at about 3.5 eV above the Fermi energy level. This peak mainly originates from the threefold-coordinated Ga atoms, where the components of atomic orbitals located within the xy plane are predominant (here the axis of a GaN nanotube is along the z direction). In contrast, the edge of the valence band is almost contributed from the N atoms, being the same as the results reported from the previous work.[16]

Unlike the case of H-1, the TDOS of the H-2 tube exhibits a broad peak ($S2$) at about 4.5 eV above the Fermi energy level [Fig. 2(c)]. This peak shows a heavy mixture of the s, p_x, p_y, and p_z orbitals of the Ga atoms. Especially, the threefold-coordinated Ga atoms attribute their atomic orbitals to this state more than the fourfold-coordinated Ga atoms. In the valence band, there is a peak marked with $S1$, which arises mainly from the threefold-coordinated N atoms. Apart from these states at the band edges, the others in the valence band are a mixture of electronic states of both fourfold- and threefold-coordinated atoms. So both $S1$ and $S2$ are surface states. Owing to the atoms arranging in order at the inner and outer surfaces of the H-3 tube, the surface states arising from these atoms form subbands within the energy gap.

IV. OPTICAL PROPERTIES

As mentioned above, the GaN nanotubes with different thicknesses have different electronic densities of states; these different electronic structures can be reflected by the absorption spectra. As we know, the imaginary parts of dielectric functions ϵ_2 determine the optical absorption.[17] We thus pay attention to the imaginary parts of dielectric functions for the GaN nanotubes. Figure 3(d) displays the dispersion of ϵ_2 as a function of photon energy for the bulk WZ GaN from our calculation, which is comparable to that in the literature.[18] Such agreement implies that the imaginary parts of the dielectric functions evaluated by using the SIESTA package in present work are reliable.

From Figs. 3(a)–3(c) we find that the calculated ϵ_2 of each GaN nanotube concerned is anisotropic, because the longitudinal component ($\epsilon_2^{\parallel}$) of the calculated ϵ_2 is strikingly different from the transverse component ($\epsilon_2^{\perp}$). Now let us focus on the calculated $\epsilon_2^{\parallel}$ curves. For the H-1 tube, a major peak marked with D is observed above the threshold energy in the $\epsilon_2^{\parallel}$ curve [Fig. 3(a)]. This peak is associated with a transition of electrons from $S1$ to $S2$ peaks that are marked in the TDOS [Fig. 2(b)] of the tube. After the threshold the $\epsilon_2^{\parallel}$ decreases discontinuously. Such a discontinuous feature stems from the transition between related peaks in the DOS. When the tube consists of two double layers (i.e., H-2), the dispersion of ϵ_2 is significantly distinct from that of the H-1 tube. There are two peaks labeled with D and B in the $\epsilon_2^{\parallel}$ curve [Fig. 3(b)]. The peak D corresponds to the transition of electrons between $S1$ and $S2$ peaks in the TDOS [Fig. 2(c)], and B corresponds to the transition between $B1$ and $B2$ peaks in the TDOS [Fig. 2(c)]. Combining this observation with the calculated density of states of the related tube, we find that the electronic states arising from the surface atoms (threefold-coordinated atoms) and bulk atoms (fourfold-

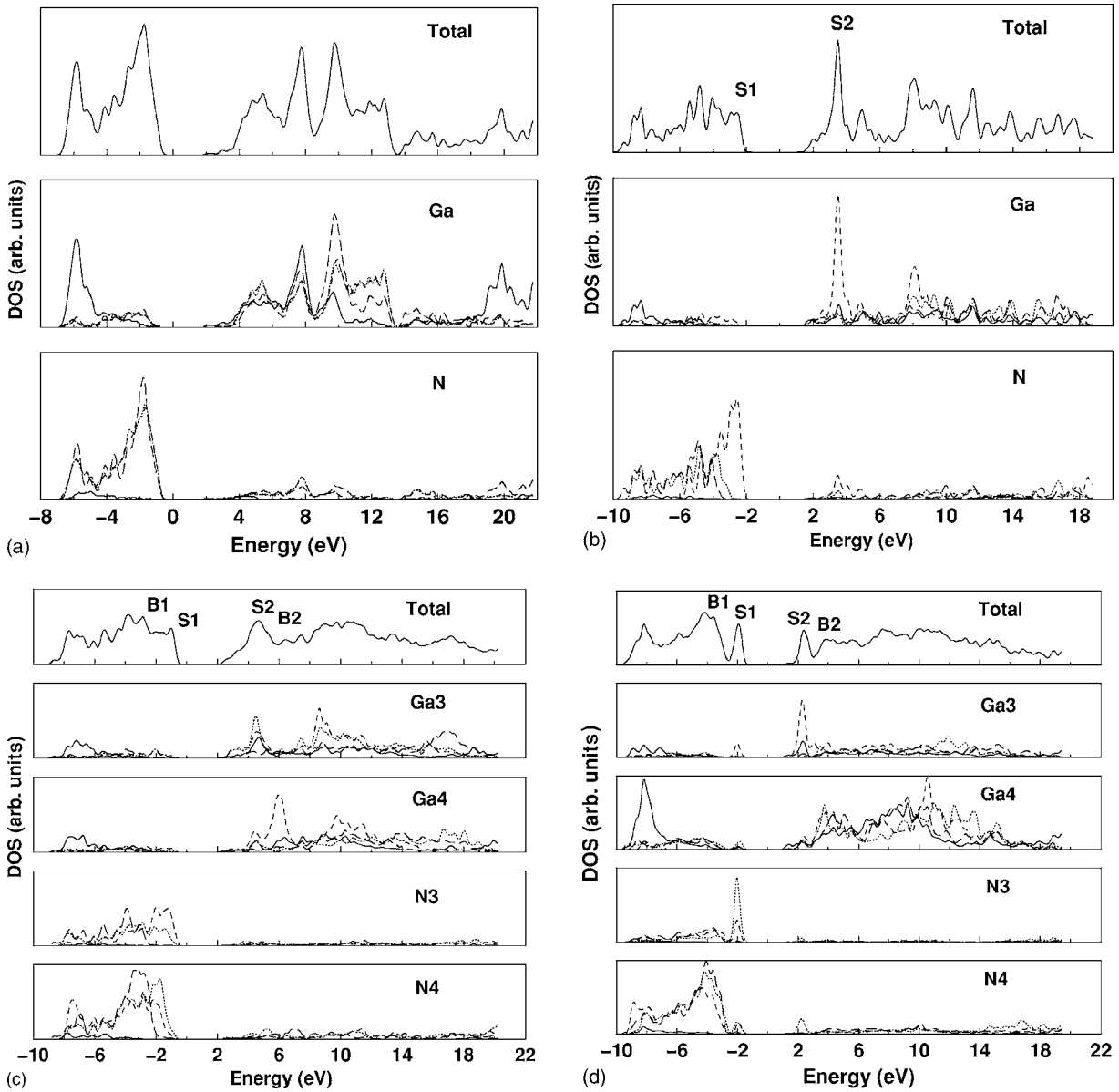

FIG. 2. The calculated density of states for (a) bulk WZ GaN, (b) H-1 tube, (c) H-2 tube, and (d) H-3 tube. Solid lines stand for the s states, dotted lines for the p_x states, dashed lines for the p_y states, and long-dashed lines for the p_z states. The Fermi energy levels E_f are all shifted to be 0 eV. Ga3, Ga4, N3, and N4 stand for the threefold- and fourfold-coordinated Ga and N atoms, respectively.

coordinated atoms) attribute to the peak D (9.58 eV) and peak B (7.94 eV), respectively. For the case of the H-3 tube, there are two main peaks at 4.23 eV and 7.46 eV [Fig. 3(c)]. The first peak corresponds to the transition between $S1$ and $S2$ peaks [Fig. 2(d)] originating from the threefold-coordinated N and Ga atoms, whereas the second corresponds to the transition between $B1$ and $B2$ peaks originating from the fourfold-coordinated N and Ga atoms. Interestingly, from Figs. 3(a)–3(c), it is found that, as the ratios of the threefold-coordinated atoms to the fourfold-coordinated atoms decrease (e.g., from the H-2 tube to the H-3 tube), the intensity of the peak D decreases with respect to the intensity of the peak B. Moreover, although a redshift of the peak B is observed as the thickness of the tube increases, the central position of this peak is still on the higher energy side relative to the major peak B in the ϵ_2 curve of the bulk WZ GaN [seen in Fig. 3(d)]. Thus, one can speculate that when the thickness of a GaN nanotube is large enough, the peak B will approach the case of the bulk WZ GaN and the intensity of peak D arising from the surface atoms will decrease largely. Note that the thickness of the single-crystal GaN nanotubes synthesized in experiment ranges from 5 to 50 nm (Ref. 8); the intensity of peak D for a realistic GaN nanotube should be very tiny. Therefore, we predict that the absorption spectrum of a realistic GaN nanotube with large thickness most probably originates from the bulk portion not from the surface. On the other hand, when the thickness of a GaN nanotube is not large enough, the feature of thickness-dependent ϵ_2 as mentioned above clues us to tailor the optical property of GaN nanotubes through controlling the thickness and lateral facets of the tubes. Such a thickness effect was also discussed in the case of the Cr-doped GaN nanotubes.[13]

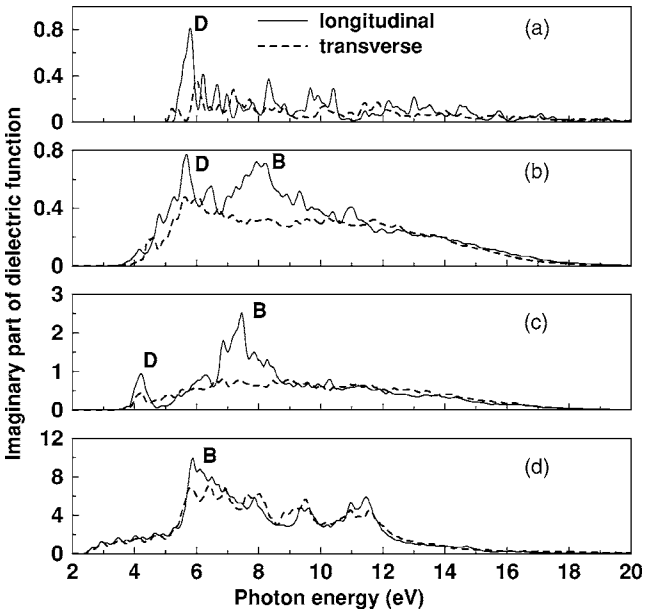

FIG. 3. The calculated imaginary parts of the dielectric functions polarized along the z direction (longitudinal component) and in the xy plane (transverse component) for (a) H-1 tube, (b) H-2 tube, (c) H-3 tube, and (d) bulk WZ GaN.

V. SUMMARY

The electronic structures and optical properties of the concerned GaN nanotubes are studied by using the density functional theory with the generalized gradient approximation. We find that the threefold-coordinated N and Ga atoms at lateral facets in a tube with hexagonal cross section give rise to surface states at both valence-band edge and conduction-band edge in the energy band, respectively. Our calculations also show two significant peaks in the ϵ_2 curves; these peaks originate from the surface atoms and bulk atoms, respectively. Moreover, the positions as well as the relative intensities of the ϵ_2 peaks are dependent on the thickness of the GaN nanotube, showing the size effect of single-crystal GaN nanotubes.

ACKNOWLEDGMENTS

This work is supported by the Fund of University of Science and Technology of China, the Fund of Chinese Academy of Science, Grants Nos. NSFC50121202 and NSFC60176024. This work is also supported by the National Basic Research Program 2006CB0L1202. We thank Haiyan He for her comments on this paper.

[1] Vincent H. Crespi, Marvin L. Cohen, and Angel Rubio, Phys. Rev. Lett. **79**, 2093 (1997).
[2] Lorin X. Benedict, Steven G. Louie, and Marvin L. Cohen, Phys. Rev. B **52**, 8541 (1995).
[3] C. Roland, M. Buongiorno Nardelli, J. Wang, and H. Guo, Phys. Rev. Lett. **84**, 2921 (2000).
[4] M. A. Pimenta, A. Marucci, S. A. Empedocles, M. G. Bawendi, E. B. Hanlon, A. M. Rao, P. C. Eklund, R. E. Smalley, G. Dresselhaus, and M. S. Dresselhaus, Phys. Rev. B **58**, R16016 (1998).
[5] J. P. Lu, Phys. Rev. Lett. **79**, 1297 (1997).
[6] Young-Kyun Kwon and David Tomanek, Phys. Rev. B **58**, R16001 (1998).
[7] J. P. Lu, Phys. Rev. Lett. **74**, 1123 (1995).
[8] J. Goldberger, R. R. He, Y. F. Zhang, S. Lee, H. Q. Yan, H.-J. Choi, and P. D. Yang, Nature (London) **422**, 599 (2003).
[9] B. Xu, A. J. Lu, B. C. Pan, and Q. X. Yu, Phys. Rev. B **71**, 125434 (2005).
[10] D. Sanchez-Portal, P. Ordejon, E. Artacho, and J. M. Soler, Int. J. Quantum Chem. **65**, 453 (1997); N. Troullier and J. L. Martins, Phys. Rev. B **43**, 1993 (1991).
[11] John P. Perdew, Kieron Burke, and Matthias Ernzerhof, Phys. Rev. Lett. **77**, 3865 (1996).
[12] S. M. Lee, Y. H. Lee, Y. G. Hwang, J. Elsner, D. Porezag, and T. Frauenheim, Phys. Rev. B **60**, 7788 (1999).
[13] Q. Wang, Q. Sun, P. Jena, and Y. Kawazoe, Phys. Rev. B **73**, 205320 (2006).
[14] H. P. Maruska, and J. J. Tietjen, Appl. Phys. Lett. **15**, 327 (1969).
[15] A. H. Mahan, R. Biswas, L. M. Gedvilas, D. L. Williamson, and B. C. Pan, J. Appl. Phys. **96**, 3818 (2004).
[16] E. Durgun, S. Tongay, and S. Ciraci, Phys. Rev. B **72**, 075420 (2005).
[17] O. Madelung, in *Introduction to Solid-State Theory*, edited by M. Cardona, P. Fulde, and H.-J. Queisser (Springer-Verlag, New York, 1978).
[18] B. Abbar, B. Bourag, G. Nouet, and P. Ruterana, Phys. Status Solidi B **228**, 457 (2001).